16th Australasian Fluid Mechanics Conference
Crowne Plaza, Gold Coast, Australia
2-7 December 2007

Strouhal Number of Naturally-Oscillating Triangular and Circular Jets

S. K. Lee, P. V. Lanspeary and G. J. Nathan

School of Mechanical Engineering
The University of Adelaide, Adelaide, South Australia, 5005 AUSTRALIA

Abstract

A nozzle consisting of an abrupt expansion into a short open-ended tube can produce a naturally-excited oscillating-jet flow. The characteristics of the oscillating jet depend on jet-orifice to chamber expansion ratio (D/d_1), chamber length-to-diameter ratio (L/D), and shape of the jet orifice. In experiments using water as a flow medium, air-bubble visualisation and signals from a pressure transducer show that a triangular-jet orifice produces aperiodic oscillation without a spectral peak. In contrast, oscillation of the circular jet has clearly visible periodicity and the spectrum has a broad peak. The circular and triangular orifices produce completely different dependence of Strouhal number on expansion ratio. For a circular orifice, Strouhal number is inversely proportional to (D/d_1-1). For a triangular orifice, Strouhal number is *directly* proportional to (D/d_1-1). The two curves intersect at an expansion ratio of 4.8, which is approximately the minimum possible expansion ratio for a circular oscillating jet.

Introduction

Partially confining the flow from an orifice with an axisymmetric chamber can produce a naturally-excited oscillating-jet flow. In the initial studies with a circular orifice, Nathan et al. [8] found that the range of confinement geometries which produce an oscillating jet is quite narrow. The diameter-expansion ratio from orifice to chamber must exceed about five, $D/d_1 \gtrsim 5$, and the length ratio of the chamber must be in the range $2.6 \lesssim L/D \lesssim 2.8$. A small lip of height $h_2 \lesssim 0.1D$ is usually attached to the chamber exit. A device with these geometric parameters is patented as the fluidic-precessing-jet (FPJ) nozzle [6]. The frequency of jet oscillation (f_p) is known as the "precession frequency" because oscillation of the jet flow resembles the precession of a spinning gyroscope. Measurements and observations of the FPJ flow [8] show that the oscillation of the jet has a broad spectral peak.

The non-dimensional time-dependent Navier-Stokes equations;

$$St_1 \frac{\partial \widehat{u}_i}{\partial \widehat{t}} + \widehat{u}_i \frac{\partial \widehat{u}_i}{\partial \widehat{x}_i} = -\frac{\partial \widehat{P}}{\partial \widehat{x}_i} + \frac{1}{Re_1} \frac{\partial^2 \widehat{u}_i}{\partial \widehat{x}_i{}^2} , \qquad (1)$$

show that characteristic frequencies of FPJ oscillation should be expressed non-dimensionally as a Strouhal number, and that the characteristic Strouhal number is a function of Reynolds number. Nathan [7] and other FPJ researchers have defined Strouhal number (St_1) and Reynolds number (Re_1) in terms of inlet-flow velocity U_1 and orifice diameter d_1 so that $\widehat{x}_i = x_i/d_1$, $\widehat{u}_i = u_i/U_1$, $\widehat{P} = P/\rho U_1{}^2$ and $\widehat{t} = t f_p$. Dimensional analysis shows that the Strouhal number also depends on parameters representing the chamber geometry and the inlet-orifice flow conditions. Mi and Nathan [5] show that, by placing a disc of diameter $\approx 0.75D$ just inside the exit plane of the nozzle, oscillation is obtained over a wide range of L/D ratios. However for this study, where there is no disc, precession requires that L/D and D/d_2 be constrained within a narrow range and only variations in expansion ratio are likely to have a significant effect on the Strouhal number; i.e. $St_1 \approx \mathbf{f}(D/d_{e1}, Re_1)$.

Mi et al. [6] found that the generation of large-scale oscillation does not require the inlet orifice to be circular. An equilateral triangular orifice (Figure 1(a)) can offer some advantages in comparison with the circular inlet of the FPJ nozzle. For example, one difficulty with the FPJ is that oscillation can spontaneously cease or can become intermittent. On the other hand, oscillation of the triangular jet is continuous and intermittency is not detected [4, 6]. Also, self-excited oscillation is obtained for expansion ratios smaller than the FPJ's lower limit of $D/d_1 \approx 5$. As a consequence, the kinetic-energy loss of flow through the oscillating-triangular-jet (OTJ) nozzle is orders of magnitude lower than the kinetic-energy loss through the FPJ nozzle. In some applications this is beneficial because it either reduces the cost of pumping the flow by orders of magnitude, or it allows a corresponding reduction in the size of the nozzle and its supporting structure.

In a parametric study of the OTJ nozzle, Lee et al. [4] have verified that continuous oscillation occurs at much smaller expansion ratios than in the FPJ. The spreading angle of flow from the OTJ nozzle is smaller than the spreading angle of the FPJ flow and it varies more gradually over a broad range of L/D ratios and inlet-expansion ratios. This allows the designer of the OTJ nozzle to specify not only a lower driving pressure than is possible for the FPJ nozzle, but also allows the designer to select a preferred jet spreading angle.

This paper compares the precession rate and spectrum of the OTJ with new and earlier measurements of the FPJ.

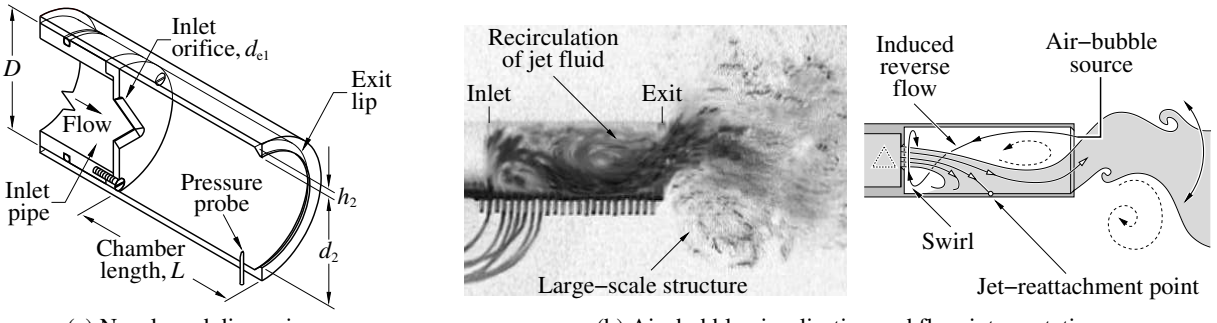

(a) Nozzle and dimensions (b) Air–bubble visualisation and flow interpretation

Figure 1: The oscillating-triangular-jet (OTJ) nozzle and its flow field (greyscales are inverted).

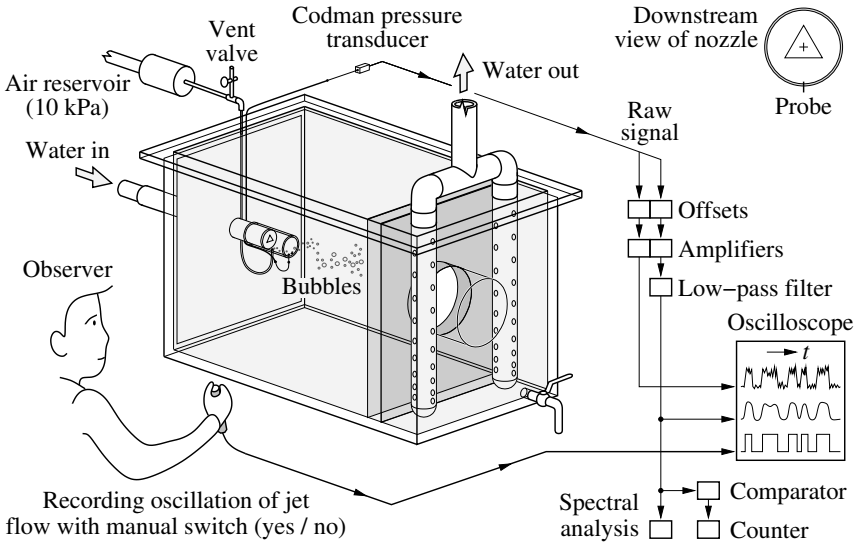

Figure 2: Arrangement of equipment for simultaneous air-bubble visualisation and pressure measurements in the OTJ flow.

Table 1: Review of FPJ Strouhal-number measurements.

Author(s) and year	Nozzle geometry			Re_1	St_1	Technique
	D/d_{e1}	L/D	d_2/D	$(=d_{e1}U_1/\nu)$	$(=f_p d_{e1}/U_1)$	
Nathan [7]	4.3[a]	~ 2.7[c]	0.9	95k→270k	0.0020→0.0026	Power spectra[i]
	9.1[a]			48k→275k	0.0007→0.0011	
	6.4[a]	~ 2.7		4k→21k	~ 0.0014	Direct observation[ii]
Nathan et al. [8]				53k→134k	0.0016→0.0017	Power spectra[i]
Mi and Nathan [5]	5.3[a]	~ 2.2[c]		28k→105k	0.0014→0.0022	
	5.3[b]			38k→98k	0.0013→0.0017	
		~ 2.3		32k→78k	~ 0.0021	
		~ 2.5		28k→109k	~ 0.0022	
	5.3[a]	~ 2.5[c]		6k→60k	0.0017→0.0032	
Wong [10]	5.1[b]	~ 2.7[c]	0.8	30k→90k	0.0014→0.0018	
Hill et al. [2]	3.8[b]	Long chamber $\gg 3.0$	–	4,406→40,738	0.0048→0.0061	Direct observation[iii]
	6.0[b]			7,046→21,077	$\sim$0.0020	
	6.4[b]			15,451→31,646	0.0016→0.0017	
	8.8[b]			40,738	$\sim$0.0010	
	14.0[b]			7,046→56,538	0.0004→0.0005	

[a] Orifice plate [b] Smooth contraction [c] Chamber includes a disc to prevent intermittency of oscillation
[i] Hot−wire signal (air); FFT spectral peak [ii] Dye visualisation (water) [iii] Particle−streak visualisation (water)

Experimental Techniques

Characteristic frequencies of the OTJ oscillation are obtained by *two* different methods of signal analysis. In both cases the flow medium is water and signals are recorded from a backward-facing pressure probe placed in the region of flow reattachment inside the chamber (Figure 1). The results are obtained at inlet-orifice Reynolds numbers in the range $40,000 < d_{e1}U_1/\nu < 100,000$, where d_{e1} is the diameter of a circle with the same area as the triangular orifice.

For the *first* method of analysis, the signal passes through a (4-pole Butterworth) low-pass filter and a comparator with adjustable threshold levels. Counting 0→1 transitions in the comparator output gives the oscillation rate. The comparator is calibrated by seeding the flow with air bubbles, directly observing the oscillation (which has a characteristic rate of less than 1 Hz), and manually counting the individual oscillations for a period of 4 minutes (Figure 2).

For the *second* method of analysis, power spectra of the pressure signal are estimated by the so called "maximum entropy method" (MEM). The maximum entropy method in statistical mechanics was first published by Jaynes [3] and was adapted for spectral estimation by Burg [1]. By definition, a power spectrum,

$$\mathbf{P}_x(f) = \int_{\tau=-\infty}^{\tau=+\infty} R_{xx}(\tau) \cdot e^{-2\pi j f \tau} d\tau \,,$$

is the Fourier transform of the autocorrelation of the data, $R_{xx}(\tau)$. In reality, only a subset of the autocorrelations is available from the experimental data. The MEM power spectrum is calculated in a way which maximises the uncertainty (or entropy) of the unavailable autocorrelations — it is obtained from the transfer function of an all-pole model of the data. The MEM has a number of advantages over the Welch [9] FFT method of spectral estimation. One of the most important is that all the spectral information is contained in just a few (in this case, five) numerical coefficients. The characteristic (or peak) frequencies in the spectrum are easily identified by converting the coefficients into "S-plane" poles. For this MEM, the signal was sampled for a duration equivalent to about 1000 oscillation events.

Inlet shape	Flow	D/d_{e1}	L/D	d_2/D	Legend
Equilateral triangle	OTJ	2.1	2.00	0.9	+
		2.5	2.25		×
		3.0	2.40		△
		3.5	2.50		□
Circle	FPJ	5.0	2.75		◯

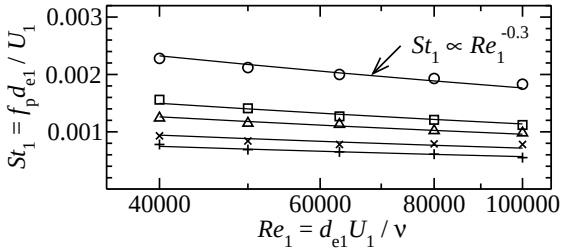

Figure 3: Direct observation of OTJ / FPJ oscillation using air bubbles in water.

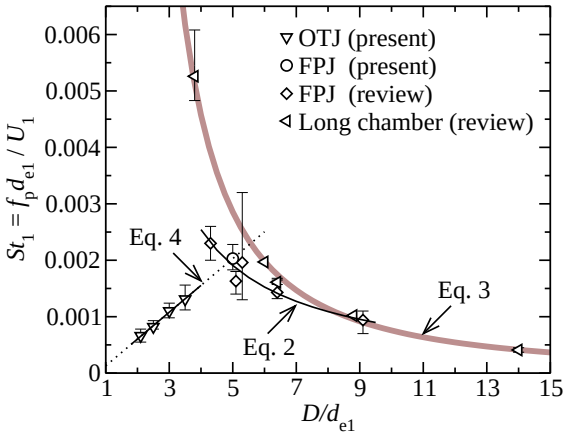

Figure 4: The OTJ / FPJ Strouhal number as function of nozzle-expansion ratio. For OTJ and new FPJ (◯) data, variation due to Reynolds number is shown in Figure 3. The review data is summarised in Table 1.

Review of FPJ Precession-Frequency Measurements

Table 1 summarises a review of previous measurements. Variations in chamber geometry, Reynolds number, and experimental technique add to the difficulties of interpreting these data. However, a least-squares fit to a relevant subset of these FPJ data [5, 7, 8, 10] and the present FPJ data (Figure 3) produces

$$St_1 = \frac{f_p d_{e1}}{U_1} = 7.6\times10^{-3}\left(\frac{D}{d_{e1}} - 1\right)^{-1},\ 4.3 \le \frac{D}{d_{e1}} \le 9.1\,, \qquad (2)$$

with r.m.s. error of 7%. The data are plotted in Figure 4 as diamonds (◇, review data) and circles (◯, present data). In another study, Hill et al. [2] have observed precession in the reattaching flow downstream of a sudden expansion into a very long chamber ($L/D \to \infty$). Hill's precession frequencies, which are shown in Figure 4 as left-triangles (◁), are different from the FPJ frequencies and fall on the curve

$$St_1 = 27.7\times10^{-3}\left(\frac{D}{d_{e1}} - 1\right)^{-1.64},\ 3.8 \le \frac{D}{d_{e1}} \le 14.0\,, \qquad (3)$$

with r.m.s. error of 5%. Hill's particle-streak visualisation experiments show that, far downstream from the sudden-expansion, the reattached "jet" from the inlet fills the cross-section of the chamber and has no easily identified characteristic frequency.

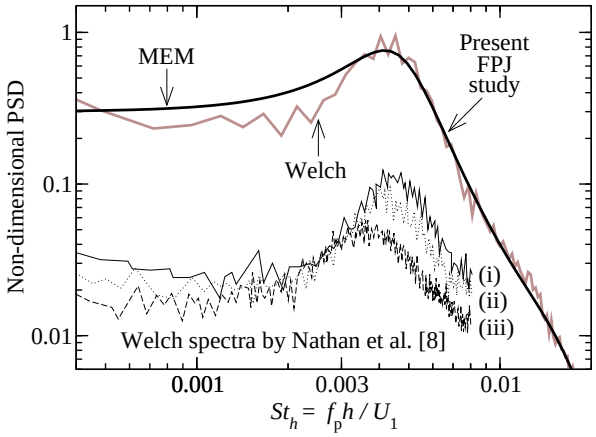

Figure 5: Comparison of power spectra from new and previous FPJ data. The Welch-method spectrum is an average of 65 256-point periodograms. The MEM spectrum has 5 poles. $Re_1 = 100,000$ at $D/d_{e1} = 5.0$. The bottom 3 curves are from hot-wire probes placed in the reattaching-jet flow [8] at Re_1 of (i) 53,100, (ii) 76,700 and (iii) 134,000 at $D/d_{e1} = 6.4$. For Nathan's data, power spectral density is unscaled.

Observed Oscillation Rate of OTJ flows

The OTJ / FPJ nozzle dimensions used for the present study are given in Figure 3. The graph in Figure 3 suggests that the oscillation rate (St_1) has a weak "−0.3" power-law dependence on Reynolds number. For studying the effects of expansion ratio, Strouhal number is simply averaged over the range of Reynolds number, Re_1. The variation due to Reynolds number is indicated in Figure 4 by the vertical error-bars. The straight-line of best fit to the OTJ data in Figure 4 is

$$St_1 = \left[475\left(\frac{D}{d_{e1}} - 1\right) + 129\right]\times10^{-6},\ 2.1 \le \frac{D}{d_{e1}} \le 3.5\,, \qquad (4)$$

with r.m.s error of 2%. The line of best fit for the OTJ data (Equation 4) and the curve of best fit for FPJ data (Equation 2) intersect at the minimum viable FPJ expansion ratio of $D/d_{e1} \approx 4.8$.

Power Spectra

The units for $\mathbf{P}_x$, the power spectral density (PSD) of pressure signal, are [pressure]^2[frequency]$^{-1}$, and so, according to dimensional analysis, non-dimensional PSD should be written as

$$\text{Non-dimensional PSD} = \frac{\mathbf{P}_x}{{q_1}^2}\cdot\frac{df}{dSt_1} = \frac{\mathbf{P}_x}{\left(\frac{1}{2}\rho {U_1}^2\right)^2}\cdot\frac{U_1}{d_{e1}} = \frac{4\,\mathbf{P}_x}{\rho^2 {U_1}^3 d_{e1}}\,, \qquad (5)$$

where $q_1 = \frac{1}{2}\rho {U_1}^2$ is the dynamic pressure at the inlet-plane of the nozzle and df/dSt_1 is the Jacobian for converting Strouhal number to frequency. The curve of best fit to the FPJ precession frequency (Equation 2) gives Strouhal number as a function of non-dimensional step height, $(D - d_{e1})/d_{e1}$, and so it suggests that the Strouhal number itself should be defined in terms of step height:

$$St_h = \frac{f_p h}{U_1} = \frac{St_1}{2}\left(\frac{D}{d_{e1}} - 1\right), \qquad (6)$$

where $h = \frac{1}{2}(D - d_{e1})$. When expressed in terms of step-height Strouhal number, Equation 2 becomes a constant:

$$St_h = 3.8\times10^{-3},\ 4.3 \le \frac{D}{d_{e1}} \le 9.1\,. \qquad (7)$$

Figure 5 shows that the spectrum of pressure signal from the detector probe has a spectral peak at the same non-dimensional

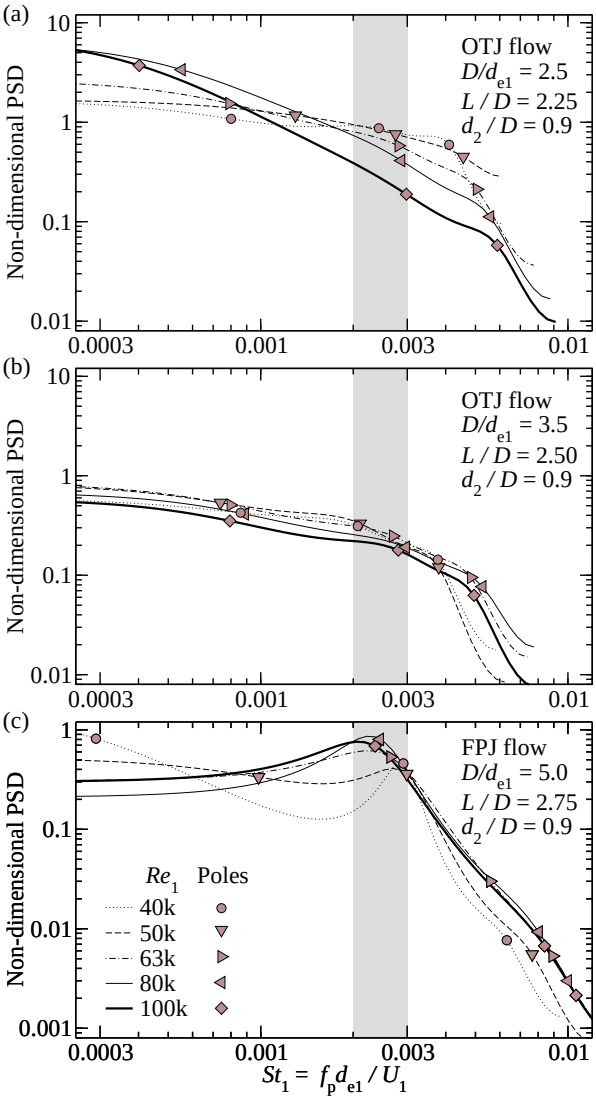

Figure 6: Non-dimensional power spectral density of OTJ / FPJ pressure-transducer signals as function of Strouhal number.

frequency (St_h) as that reported in Figure 14 of Nathan et al. [8]. However, noise and lack of frequency resolution can make interpretation of FFT-based power spectra more difficult than interpretation of MEM spectra. The MEM spectra for the OTJ and FPJ flows are presented in Figure 6.

Figure 6(c) shows that, for spectral Strouhal numbers in the range 0.003 to 0.008, the non-dimensional spectra of FPJ precession become essentially independent of Reynolds number as Re_1 exceeds 63,000. The Strouhal number of the spectral peak follows the trend of the observed oscillation frequency, and has a weak dependence on Reynolds number given approximately by $St_1 \propto Re_1^{-0.3}$. The FPJ has an expansion ratio of $D/d_{e1} = 5.0$. With the OTJ, oscillation occurs at smaller expansion ratios. However, spectra of OTJ oscillation (Figure 6(a, b)) show that, as OTJ expansion ratio decreases, independence from Re_1 is lost. For $D/d_{e1} = 3.5$, the dependence on Reynolds number is weak; it takes the form of a vertical shift in the spectrum of about 30% over the Reynolds-number range $40,000 \leq Re_1 \leq 100,000$. At smaller expansion ratios ($2.1 \leq D/d_{e1} < 3.5$), the spectrum varies with Reynolds number in a much more complex manner.

The signal from the OTJ is aperiodic and the power spectrum has no peak. Poles of MEM spectra from OTJ data fall into three widely separated groups at low, middle and high frequencies. The middle group of poles ($0.002 \lesssim St_1 \lesssim 0.003$) are near the FPJ oscillation frequency given by Equation 2. The low-frequency poles are scattered around the observed OTJ Strouhal numbers, which are shown as downward-pointing triangles ($\bigtriangledown$) in Figure 4. The high frequency poles are close to the filter cut-off frequency.

Conclusions

Strouhal number of OTJ and FPJ oscillation is obtained from air-bubble visualisation and power spectra of pressure measurements in the nozzle chamber. FPJ Strouhal number is inversely proportional to expansion ratio D/d_{e1} and the power spectrum has a broad peak. The OTJ Strouhal number observed in flow visualisation is different from that of the FPJ. It is directly proportional to expansion ratio and there is no corresponding spectral peak. The two (FPJ and OTJ) Strouhal-number curves intersect at $D/d_{e1} = 4.8$, which is approximately the minimum viable expansion ratio of the FPJ.

Acknowledgements

The support of the ARC and FCT is gratefully acknowledged. Special thanks to A/Prof. R. M. Kelso for proof reading this article and to Mr. G. Osborne for preparing the pressure probe.

References

[1] Burg, J. P., Maximum entropy spectral analysis, in *Proceedings of the thirty-seventh meeting of the society of exploration geophysicists*, Oklahoma city, Oklahoma, 1967.

[2] Hill, S. J., Nathan, G. J. and Luxton, R. E., Precession in axisymmetric confined jets, in *Proceedings of the Twelfth Australasian Fluid Mechanics Conference*, Sydney, New South Wales, Australia, 1995, 135–138.

[3] Jaynes, E. T., Information theory and statistical mechanics, 1, *Physical Review*, **106**, 1957, 620–630.

[4] Lee, S. K., Lanspeary, P. V., Nathan, G. J., Kelso, R. M. and Mi, J., Low kinetic-energy loss oscillating-triangular-jet nozzles, *Experimental Thermal and Fluid Science*, **27**, 2003, 553–561.

[5] Mi, J. and Nathan, G. J., Self-excited jet-precession Strouhal number and its influence on downstream mixing field, *Journal of Fluids and Structures*, **19**, 2004, 851–862.

[6] Mi, J., Nathan, G. J., Luxton, R. E. and Luminis Pty. Ltd., Naturally oscillating jet devices, Australian Patent Office, Patent Application No. PP0421/97, 1998.

[7] Nathan, G. J., *The enhanced mixing burner*, Ph.D. Thesis, The University of Adelaide, Department of Mechanical Engineering, Adelaide, South Australia, Australia, 1988.

[8] Nathan, G. J., Hill, S. J. and Luxton, R. E., An axisymmetric 'fluidic' nozzle to generate jet precession, *Journal of Fluid Mechanics*, **370**, 1998, 347–380.

[9] Welch, P. D., The use of fast Fourier transform for the estimation of power spectra: A method based on time averaging over short, modified periodograms, *IEEE Transactions on Audio and Electroacoustics*, **AU-15**, 1967, 70–73.

[10] Wong, C. Y., *The flow within and in the near external field of a fluidic precessing jet nozzle*, Ph.D. Thesis, The University of Adelaide, School of Mechanical Engineering, Adelaide, South Australia, Australia, 2004.